

# An example study using conventional 3D seismic data to delineate shallow gas drilling hazards from the West Delta Deep Marine Concession, offshore Nile Delta, Egypt

Andy Sharp<sup>1,2</sup> and Andy Samuel<sup>1,3</sup>

<sup>1</sup>BG Egypt, 23 Road 216, Digla, Maadi, Cairo, Egypt

<sup>2</sup>Present address: Apache North Sea Limited, Alba Gate, Stoneywood Park, Stoneywood Road, Dyce, Aberdeen AB212 7DZ, UK (e-mail: andy.sharp@apachecorp.com)

<sup>3</sup>Present address: BG Group, 100 Thames Valley Park Drive, Reading, Berks RG6 1PT, UK (e-mail: andy.samuel@bg-group.com)

**ABSTRACT:** This paper details a study that was completed at the end of 1999 to investigate the suitability of using existing, high quality, conventionally processed 3D seismic data (hereafter 3D data) to replace specifically commissioned 2D seismic site survey data (hereafter 2D site data). For this study, three wells from an existing dataset of six in the West Delta Deep Marine Concession, offshore Egypt (WDDM) were investigated. A prescriptive workflow was developed using the 3D data and the results compared to those obtained from a conventional previously commissioned 2D digital site survey dataset. For this dataset from WDDM, the results obtained from the 3D data and the 2D data were similar, the main difference being that more numerous, smaller probable hazards were prognosed by the 3D data. After undertaking this investigation and following an independent review of the results, a recommendation was made to operate the 2000 WDDM drilling campaign using hazard prognosis from the conventional 3D data, i.e. not to acquire well-specific, new digital site surveys. This recommendation was followed and five exploration wells were drilled in 2000 with no specific, digital site survey data being acquired. No safety, operational or environmental implications were encountered as a result of this replacement and significant operational savings accrued to the operating partnership.

**KEYWORDS:** Egypt, shallow gas, 3D, Nile Delta

## BACKGROUND

The West Delta Deep Marine concession is a large exploration licence located in the present-day Nile Delta, offshore Egypt (Fig. 1). The concession covers 6125 km<sup>2</sup> of the northwestern margin of the Nile Delta Cone. This concession was initially operated by BG International (50%) and partner Edison Gas (50%). Following the successful exploration and appraisal programme and signing of a Gas Sales Agreement, operatorship has passed to Burullus Gas, a Joint Venture operating company composed of the Egyptian General Petroleum Company (50%), BG International (25%) and Edison Gas (25%). Recent exploration success has been focused on the Pliocene slope channel play, with a total of 13 successful exploration wells drilled in WDDM over the past five years. Further details of the specific nature of these exploration discoveries can be found in Samuel *et al.* (2003).

At the time of completion of this study (end-1999), the WDDM Concession had been explored in a successful six-well appraisal drilling campaign based primarily around high quality 3D data. The wells drilled at that point in time were: Scarab-1 and -2; Saffron-1 and -2, Serpent-1 and Simian-1. There had been no instances of shallow water flows or overpressured

shallow gas anomalies being encountered in any of the six wells drilled. Each of the six wells had been assessed for drilling hazards using a conventional 2D digital seismic and analogue site survey. The main product of these site surveys had been the prognosis of high risk gas anomalies based on anomalously high seismic amplitude response. Where such a response was observed and coincident with the well trajectory, the well was moved. Such a movement had been necessary in only one of the exploration wells (Simian-1) to date. At the time of the study, two large 3D seismic surveys had been acquired in 1996 (hereafter WDDM96 3D) and 1998 (hereafter WDDM98 3D). The location of these 3D surveys is shown in Figure 1. All of the seismic data used in this study are full offset stacked. The seismic data used in this analysis had been processed to preserve true amplitudes. Data clipping was minimized when loading the data, again to preserve the high amplitude data values.

Given the background of the WDDM concession at the end of 1999, six wells drilled with no major operational problems; high quality seismic data, deep (>500 m) water depths and planning for an extensive 2000 drilling campaign of five wells, this point in time seemed a sensible opportunity to review

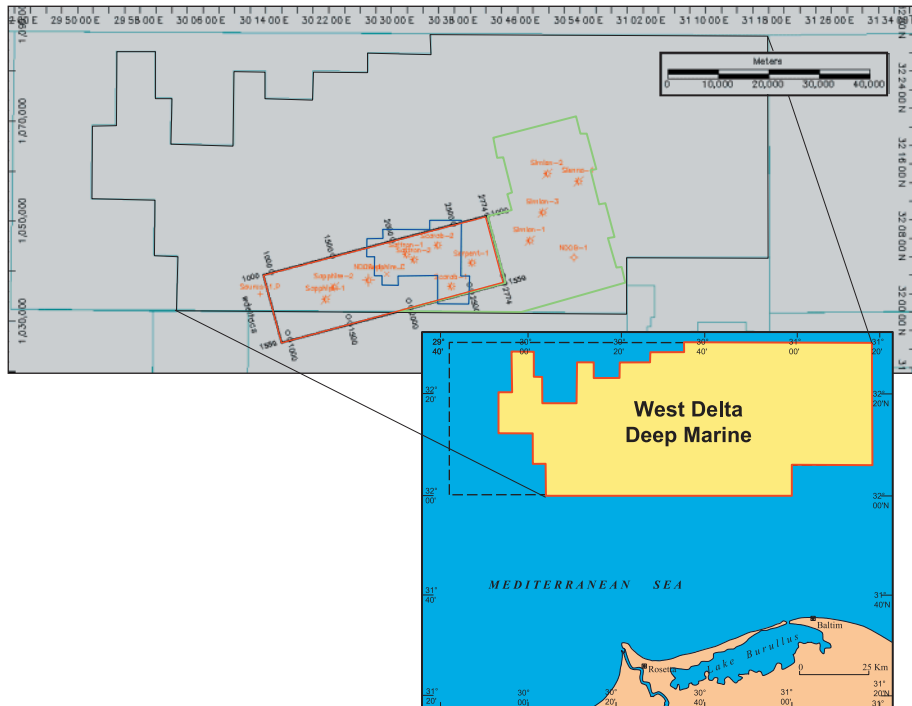


**Fig. 1.** Location of the WDDM Concession relative to the Egyptian coast. Zoomed in area shows WDDM Concession (black), 1996 3D seismic area (red), 1998 3D seismic area (green) and Scarab-Saffron development lease (blue).

whether 3D data could be used as a replacement for 2D data? The suitability of the 3D data was considered to be further enhanced by consideration of the nature of many of the shallow gas hazards in WDDM. Many of the hazards observed are small and isolated and it was thought that these could be best identified with high areal sampling, such as that provided by the 3D data.

## INTRODUCTION

It is accepted that in deep-water areas with good quality 3D data, precedents have been set for the necessary regulatory approvals to be granted for 3D data to be used exclusively for pre-drilling hazard assessment of deep-water sites (Campbell 1999; Hill 1996). Some of the reasons for this suitability of the 3D data are outlined in the UKOOA (2000) guidelines for deep-water operations and include:

- the near seabed seismic data being of higher quality than in shallow-water areas;
- the ability to locate the site survey in a regional context;
- the resolution of good quality 3D data being similar to dedicated bathymetric surveys;
- regional water bottom trend derivations.

Further caveats on the use of such 3D data are that it should be used in areas where a database of drilling experience exists and on a case-by-case basis. Campbell (1999) details the following key observations:

‘(3D) Analyses are robust and areal sampling points are typically a few tens of meters apart in all directions (compared to typical MMS required 2D geohazards data, where survey lines are typically 1000 ft apart)’.

‘A question of risk. Within the bounds of applicable regulations, the decision to use 3D data alone for deep water predrilling geohazards assessment is not simply a question of technical adequacy, but is a question of financial risk. In the end, a business decision must be made as to how much risk is acceptable. How much insurance do I want to buy? Thus, the limitations and benefits of 3-D data vs. other data must be

considered on a case by case basis and coupled with an operators risk philosophy to make a decision’.

Some of the associated benefits of using available 3D data are:

- available in a timely fashion, ‘off the shelf’ for new well locations;
- 3D migration algorithm used – truer spatial migration than 2D data migration;
- larger airguns used, lower frequency but better energy penetration;
- longer streamer offsets used, important in deeper water;
- high density spatial sampling (typically  $25 \times 25$  m grid or better);
- meaningful 3D amplitude extractions can be produced for true areal extent of hazards;
- flexibility in case of problems with chosen site survey area;
- data polarity should be known and understood;
- well locations can be placed in regional context, for example, consider Figure 2, a rendering of water bottom state in WDDM96 dataset;
- interpretation exclusively on digital workstations;
- relatively low cost, as it is pre-existing data;

Figure 2 is a classic example of the benefits of locating wells in a regional context. Several features can be observed on this image, which was obtained by running coherency analyses and extracting coherency at water bottom. These features include the surface expression of a shale/mud diapir, pockmarks and major slump horizons. It would be near impossible to interpret these features in a regional context without the 3D image, using only a conventional  $2 \times 2$  km site survey data. A further example of using water bottom 3D seismic images for early detection and delineation of both surface and subsurface hazards prior to the acquisition of high-resolution ‘hazard’ surveys is detailed by Long *et al.* (1999).

Some considerations of conventional 2D data are:

- higher frequency airguns are used, yielding better resolution, both vertically and areally;

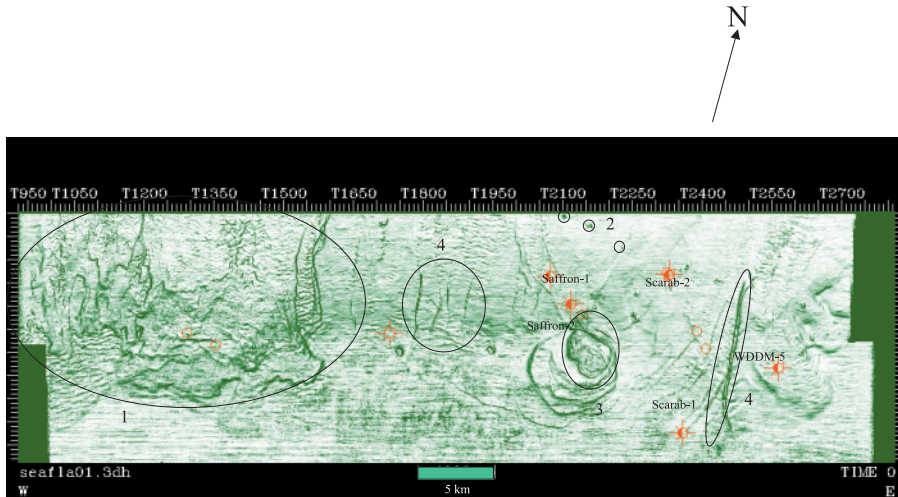


**Fig. 2.** Coherency extraction at seabed showing regional context of wells. Annotated features are: 1, slump/slope failure with evidence of mass flow deposits and fault scarp development; 2, small gas escape pockmarks; 3, surface expression of gas chimney/shale diapir displaying recent movement and sediment shedding in northwest and southeast directions; 4, ephemeral channels of different sizes.

- site survey data interpretation is often completed using paper seismic and basemap data (Hill 1996). This manual technique had been used for all the 2D data analyses in WDDM. Furthermore, in these WDDM examples, different interpreters had been used for each of the different surveys;
- denser velocity picks, leading to better constrained depth conversions.

Another alternative approach considered was reprocessing of the conventional 3D seismic data using short offset traces (Cowland 1996). However, investigation of this methodology was deferred until a rigorous evaluation of the existing 3D data had been completed.

### CALIBRATION

Three existing well locations with conventional 2D site surveys and many anomalous reflections over them were mapped using the 3D data. The results from the 3D data were compared with the existing results from the dedicated 2D data. The wells used for this comparison were: Scarab-1, Saffron-2 and Simian-1. Two of these wells (Scarab-1 and Saffron-2) lie within the WDDM 1996 3D seismic volume and the third, Simian, lies within the WDDM98 3D. The results and methodology of this comparison are described below.

To quantify the seismic data and relate amplitudes to probable gas sands in the shallow section, two horizons were investigated in detail around the Scarab-1 well. These horizons were interpreted at a stratigraphic level that included high amplitude seismic events interpreted to represent gas-charged sands. These horizons were manually picked on every inline and crossline over a limited area of interest to ensure a high quality interpretation. The two horizons were chosen at differing levels below mudline ('shallow' *c.* 150–200 ms and 'deep' *c.* 600 ms below mudline) in an attempt to ensure that the calibration of the amplitudes was over a wide temporal window that included times that were expected to include a range of probable gas hazards.

An arbitrary 3D seismic line over the shallow level prognosed gas sand is shown in Figure 3. The location of this arbitrary line is shown in Figure 4, along with amplitude extractions which are discussed further below. The water bottom 'hard' seismic pick is shown as a thin red horizon and is interpreted on a red trough. The top of the hazard-prone horizon has been picked on a black peak as a 'soft' kick and is coloured yellow. It is apparent on examining the data closely that the high amplitudes associated with the red trough below

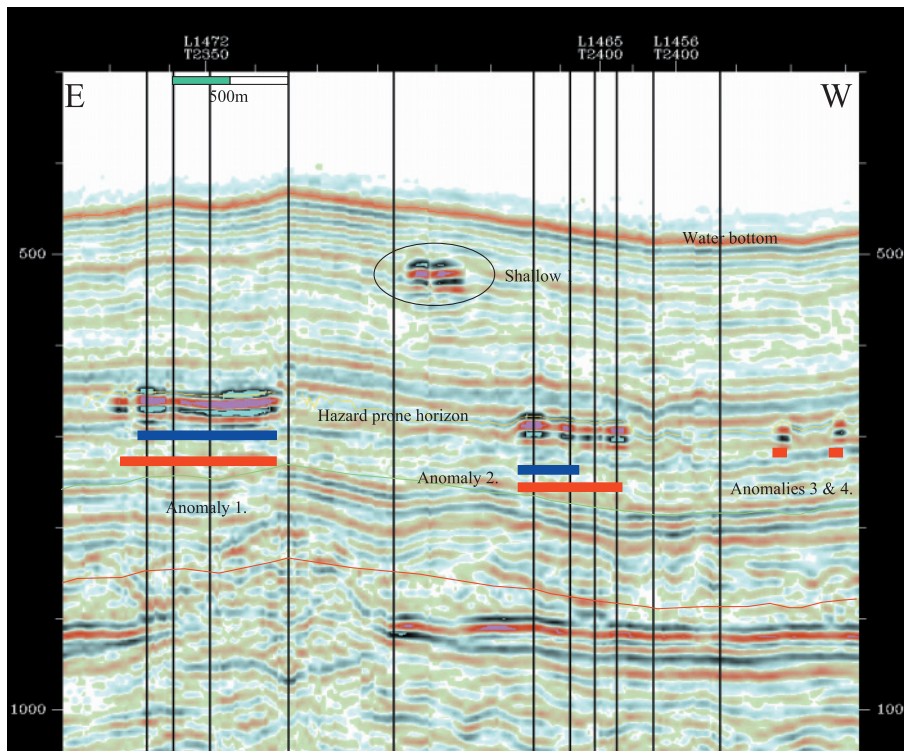
the horizon pick are more laterally extensive and brighter than both the top and base peak amplitudes. It is suggested that this observation may be related to the phase of the data. These seismic data have been zero phased based on well and seismic data from the prime area of interest around the reservoir sections which are deeper (1500+ ms below mudline) than the prognosed hazards discussed here. Well-based zero phasing of the shallow data could not be undertaken as no wireline data have been acquired in the top hole sections.

Figure 4a shows a maximum positive amplitude extraction from +10 ms to –10 ms around the yellow horizon shown in Figure 3. Figure 4b details a maximum absolute amplitude extraction from +10 ms to +30 ms around the yellow horizon shown in Figure 3. This +10 ms to +30 ms window is targeted to extract the maximum magnitude associated with the negative data troughs. A maximum magnitude extraction was chosen so that the positive amplitudes of the peak and negative amplitudes of the trough data could be compared directly. The colour bar used for the displays is shown in Figure 4c. This colour scheme has been chosen to show low amplitudes as navy blue for low emphasis, a yellow transition for intermediate amplitudes and red to accentuate high amplitudes. The colour bar is also cropped at amplitude 64, meaning data above these values appear black (in the centre of bright anomalies).

The observations noted above suggested that the maximum absolute amplitude extraction gave the highest amplitudes and the largest lateral extent, when maps were compared using the same colour bar. To understand this difference, the sections of the arbitrary line in Figure 4 which relate to high amplitude, red anomalies have been highlighted in green. These areas have then been backplotted onto Figure 3, blue for areas which were highlighted by the maximum positive (–10 ms to +10 ms) and red for areas highlighted by the maximum absolute amplitude (+10 ms to +30 ms). As expected, using the same colour bar, the red areas are more extensive and also seem to show more correspondence with particular amplitudes associated with structural closures, e.g. the two bright pockets to the right of Figure 3.

As a further QC of the amplitudes, the water bottom and top horizon surface times were depth converted to produce depth horizons. The depth conversion used a water velocity derived from temperature–salinity dips and a mudline to top horizon velocity of 1500 m s<sup>–1</sup>, 1600 m s<sup>–1</sup> or 1800 m s<sup>–1</sup> as sensitivities. The interval velocity values were chosen to include the full range of typical shallow velocities expected in the WDDM wells from deeper checkshot information. Three top





**Fig. 3.** Arbitrary line detailed in Figure 4 and amplitude extents as discussed.

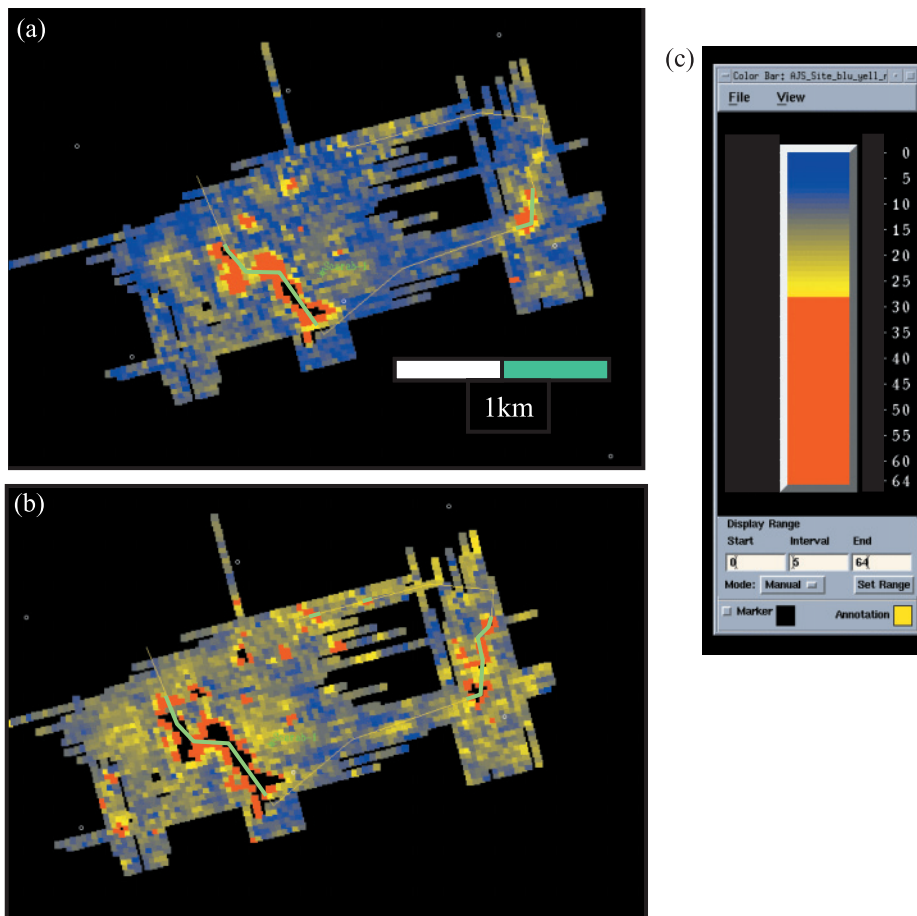


**Fig. 4.** (a) Maximum positive amplitude extraction from  $-10$  ms to  $10$  ms. (b) Maximum absolute amplitude extraction from  $+10$  ms to  $+30$  ms. Both amplitudes from hazard-prone horizon detailed in Figure 3. Same colour bar (c) applied to both images. Arbitrary line location shown in yellow and high amplitude values backplotted in Figure 3 shown in green.

depth grids were generated and the differing contours related to anomaly 1 in Figure 3 are shown in Figure 5. The contours are overlain on the maximum negative amplitude values. The three

closing structure cases all show a good, but not perfect, relationship with the extent of anomaly 1. This good structural–amplitude match, considered in conjunction with the flat

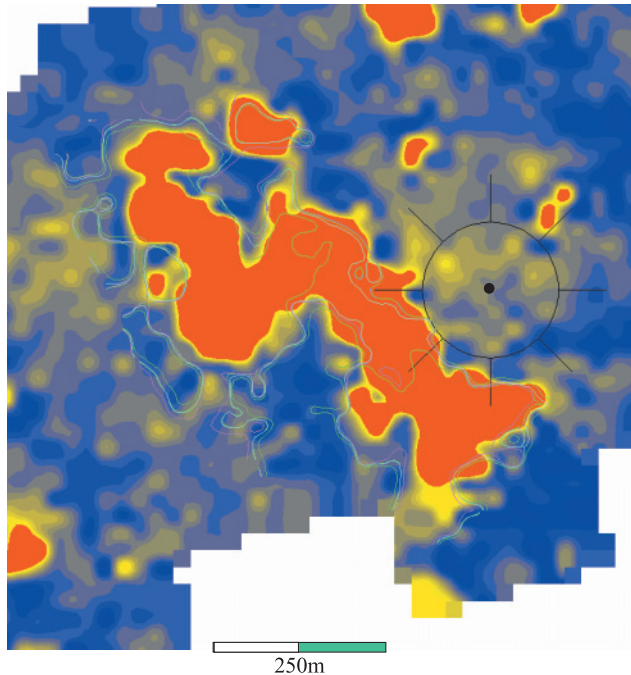


**Fig. 5.** Anomaly 1 maximum amplitude extraction from +10 ms to +30 ms of hazard-prone horizon detailed in Figure 3. Overlain best structural closure corresponding to fixed water velocity and varying sediment interval velocities of  $1500 \text{ m s}^{-1}$ ,  $1600 \text{ m s}^{-1}$  and  $1800 \text{ m s}^{-1}$ . Scarab-1 well location also detailed.

basal nature of the event, suggests that the anomaly is, in fact, a structural accumulation that is likely associated with a gas-charged sand. One other key point to note from Figures 3 and 4 are the sizes of anomalies 3 and 4. In map view, several of these anomalies cover an area of  $25 \times 50 \text{ m}$  (two seismic bins). It is highly likely that these anomalies or something similar would not be intersected by a grid of 2D seismic data. The sparseness of 2D data could be problematic if the well location was required to be moved and emphasizes the relative flexibility of the 3D seismic data.

Figure 6 shows the results of the same workflow over the deeper horizon near the Scarab-1 well. Figure 6a is an arbitrary seismic section from the line with the second, deeper horizon shown as a thin red interpretation. Figure 6b shows the maximum absolute amplitude extraction from +10 ms to +30 ms below the horizon. Sections of the seismic line shown in green are backplotted to the seismic line as red rectangles.

Again, there is excellent correspondence between what would be interpreted as probable gas hazards in section and areas delineated by red, or above, amplitudes in the map

display. These two examples suggested that the colour bar and cut-offs derived for these seismic horizons were robust and realistic over the time intervals investigated. The amplitude-based nature of the results lends itself to integration into a more mechanistic, less labour-intensive workflow.

## WORKFLOW

Maximum absolute negative amplitude extractions were generated over a 100 ms window, starting from 10 ms parallel below the seafloor. This '10 ms below seafloor' line was chosen as a starting point to avoid any contamination of the extraction by sidelobes of the high amplitude water bottom event. This process resulted in several horizons extracted between 10 and 110 ms, 110 and 210 ms, 210 and 310 ms and so on, below the seafloor. Figure 7 shows four of these amplitude extractions around the Scarab-1 well location from 10–110 ms, 110–210 ms, 210–310 ms and 610–710 ms below water bottom.

All the figures displaying amplitude extractions are presented using the same colour bar. As described above in the calibration section, this colour bar was very carefully chosen and is consistently applied. Examination of the 110–210 ms and 210–310 ms extractions demonstrates clearly that all of the anomalies investigated by the first horizon are delineated. Similarly, examination of the 610–710 ms extractions shows clearly that all of the anomalies investigated by the second horizon are delineated. One further calibration point is the anomaly in Figure 3 which is labelled Shallow 1. Inspection of Figure 7a, the 10–110 ms window, shows this anomaly is also well defined.

For each 100 ms windowed amplitude extraction, a polygon was drawn around each significant red anomaly. The criteria for judging 'significance' combined anomaly size and planned well proximity. Examples of some polygons are shown in Figure 7e. If an anomaly was near to a proposed well it was more significant than a similar-sized anomaly more distal from the proposed location. These multiple polygons from each time window were then stacked to form a 'pseudo' site-survey derived from 3D data. A first observation is that these 'pseudo site-surveys' generated from 3D data contain many anomalies. Two maps were generated for each proposed well location. Two maps were necessary due to the number of anomalies mapped for each well. The first map contains the shallow anomalies from the 10–110 ms, 110–210 ms and 210–310 ms intervals. The anomalies generated from each time window are coloured red, green and blue, respectively. The second contains the deeper anomalies from the 310–410 ms, 410–510 ms and 510–610 ms intervals. These deeper anomalies are coloured pale blue, lilac and yellow, respectively. An

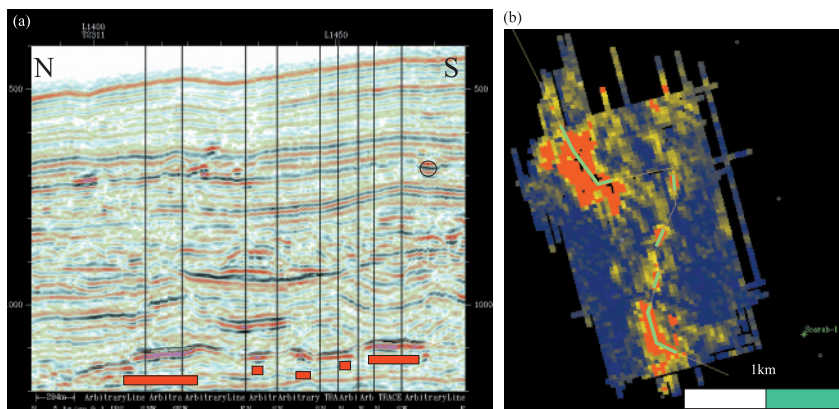


**Fig. 6.** (a) Arbitrary seismic line and (b) location of line (fine yellow) overlain on maximum absolute amplitude extraction from +10 ms to +30 ms. Bold green areas are backplotted in red on the arbitrary line. Colour bar as Figure 4c.



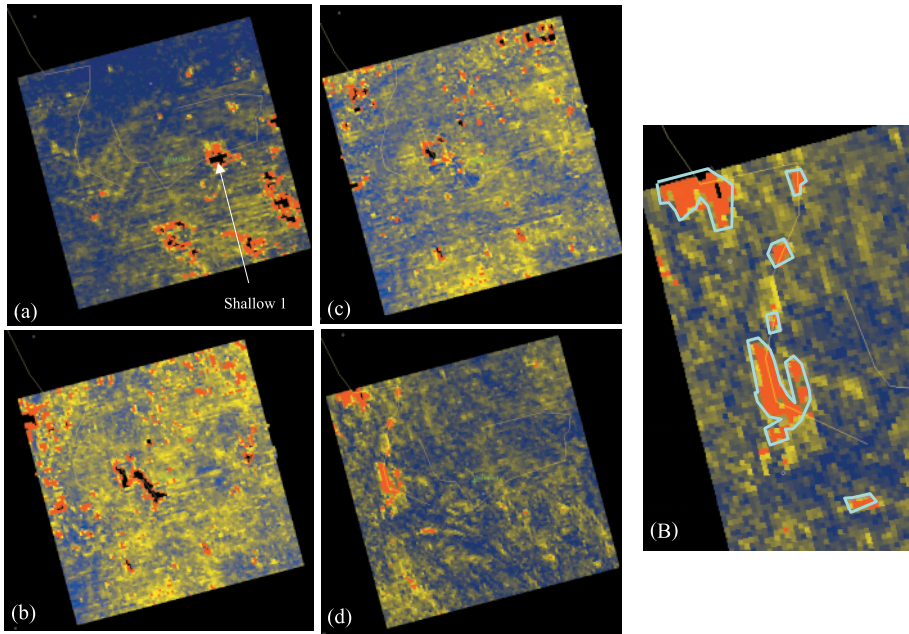


**Fig. 7.** Maximum absolute amplitude extractions from (a) 10–110 ms, (b) 110–210 ms, (c) 210–310 ms and (d) 610–710 ms. All extractions defined from parallel to seabed and extracted in a  $2.5 \times 2.5$  km inline-crossline orientation cube around the Scarab-1 well. Colour bar as Figure 4c. (e) Details of some of the polygons which were digitized for this particular extraction from the 610–710 ms time window.

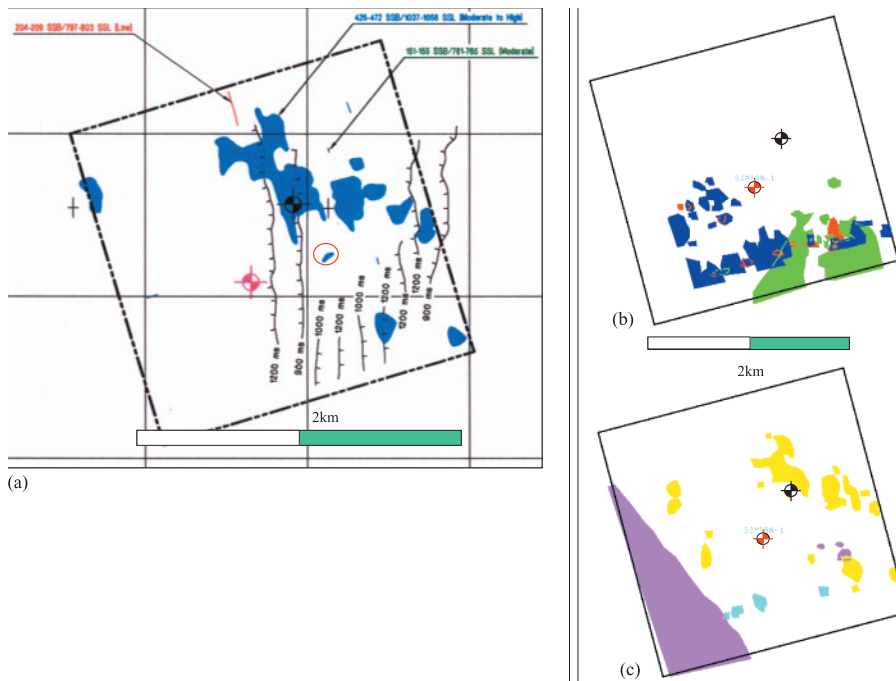


**Fig. 8.** (a) Site survey around Simian-1. (b, c) Digitized polygons from pseudo-site survey from 3D data over the same area: (b) polygons generated from 0–110 ms (red), 110–210 ms (green) and 210–310 ms (blue) windows below water bottom, respectively; (c) polygons generated from 310–410 ms (pale blue), 410–510 ms (lilac) and 510–610 ms (yellow) windows below water bottom, respectively. Well locations are the same in all figures. The black symbol is the initial proposed well location and the red symbol the revised location following coincidence of the initial location with a prognosed shallow gas hazard.

example of the result from this type of analysis is shown in Figure 8.

This ‘survey’ was then compared to the conventional site survey dataset mapped by the existing site survey contractor from 2D site data. An example comparison is shown in Figures 8b and 8c for the Simian-1 well. Both have the two proposed well locations highlighted, a red well symbol showing the location of a well which was prognosed to be a hazard-free well location from the 2D data and a black well symbol which was prognosed to be a hazardous location from the 2D data. This example is illustrated as there are few anomalies and a direct comparison is reasonably straightforward. It is readily apparent that there is an excellent match between the two results. The only near-well anomaly mapped by the 2D data and not delineated by the 3D data is shown ringed by a red ellipse in the Figure 8a. Re-investigation of the 3D amplitude

extractions explained this discrepancy – the anomaly had not been polygonized as it had been adjudged ‘insignificant’, being small and relatively distal from the well. To reiterate, one further, key observation is that the 3D data interpretation obviously delineates more numerous, smaller probable hazards due to its high density areal sampling than the digital site survey data.

The results are similar, although not as clear due to there being more hazards mapped from the 3D data, for the Scarab-1 and Saffron-2 wells. Again, for both these wells, the 3D data interpretation delineated more numerous, smaller probable hazards due to its higher density areal sampling.

Also extracted as part of the suggested workflow are coherency extractions at 0, 100, 200, 300, 400 and 500 ms two-way time (TWT) below the water bottom. The purpose of these displays is to provide an easily comprehensible quick

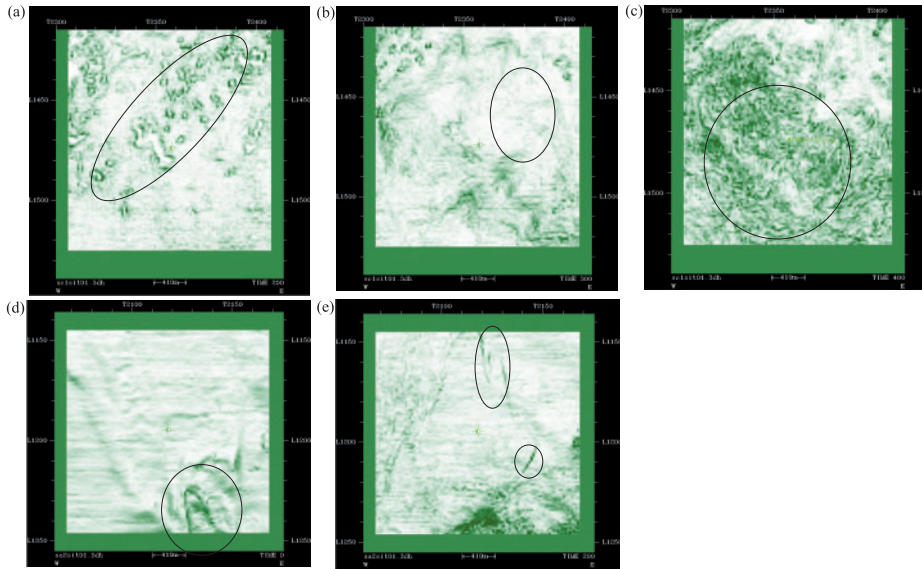


**Fig. 9.** Coherency extractions parallel to water bottom around the Scarab-1 well, with highlighted features outlined at: (a) 200 ms below water bottom, showing pockmarks; (b) 300 ms below water bottom, with parallel-bedded seismic; and (c) 400 ms below water bottom chaotic seismic. Coherency extractions at (d) water bottom around the Saffron-1 well, showing slumps at water bottom and (e) 200 ms below water bottom, showing faults. Area of data coverage is  $2.5 \times 2.5$  km. Inlines and crosslines are rotated to E-W and N-S in this display.

overview to determine the structural and seismic character within the dataset. Haskell *et al.* (1999) detail numerous features which can be recognized from coherency data. Some examples of the quality of the coherency data are shown by the annotated results in Figure 9 around the Scarab-1 and Saffron-2 wells. These figures are coloured such that incoherent events (such as faults) are dark green. Laterally continuous events, such as parallel-bedded seismic data are coloured white to pale green. Figure 9a is particularly interesting as it shows details of gas escape pockmarks around the Scarab-1 well location associated with the various anomalies already discussed from horizon 1, earlier. Again, it seems unlikely that all of these anomalies would be delineated with a conventional 2D site survey grid. Another point to note from the coherency extractions around the Scarab-1 well is the direct relationship between light-coloured, high coherency areas (Fig. 9b) and dark-coloured, incoherent areas (Fig. 9c). This relationship can be directly attributed to the seismic character, with the light areas representing parallel-bedded seismic data and the dark areas representing slumped, chaotic seismic bedforms.

Figures 9d and 9e show two coherency extractions from around the Saffron-2 well location. Here, clear examples illustrating slumping at water bottom and near-surface faulting are well delineated from the coherency data.

A final, more direct way to compare 2D site data and conventional 3D data is provided by seismic sections over the same location. When making this comparison it is important to consider the navigation associated with each of these datasets. The 3D seismic data have been acquired using DGPS to locate the vessel and RGPS between vessel and tail buoys, as well as an acoustic network along the streamer. The site survey data have been acquired using a single DGPS on the vessel and no in-water streamer positioning. Further, the 3D data are migrated using 3D operators whilst the 2D site data can, by default, only be migrated in a 2D sense.

Figure 10 compares a 2D seismic site survey seismic line across the Scarab-1 well and a 3D line over the same, nominal location. There are several observations worth noting. It is obvious that the site survey data have slightly higher vertical resolution. However, it is equally apparent that the 3D data are superior in other areas. For instance, the site survey data have limited lateral continuity of deeper horizons (due simply to fold tapering off). Obviously, there are no migration edge effects on the 3D data when compared to the 2D data.

The vertical resolution limitations of the 3D data can be easily understood by examining Figure 11 which shows the frequency of typical site survey data and samples from the WDDM96 and WDDM98 datasets. All of these data have been derived from 200–400 ms below mudline at the same locations for both datasets. Black, vertical lines have been drawn to show the 20 and 80 Hz frequency limits. The site survey data have relatively higher energy levels in the 80–125 Hz spectrum, which will provide better vertical resolution. Considering the peak frequency of the data, the digital site survey data have a peak frequency of  $\approx 65$  Hz whilst that of the 3D data is  $\approx 45$  Hz. Using an appropriate velocity of  $1600 \text{ m s}^{-1}$ , these peak frequencies equate to wavelengths of  $\approx 25$  m and  $\approx 35$  m for the 2D and 3D data, respectively. Using a  $\lambda/30$  bed thickness detection criterion, as suggested in Sheriff (1991), results in theoretical bed thickness detection criteria of  $>0.8$  m and  $>1.2$  m for the 2D and 3D data, respectively. The 1.2 m for the 3D seismic data is consistent with Hills (1996) observation that 1 m gas sands within a young section (as in WDDM) can be detected if not resolved. This 1 m figure is often quoted as the limit of resolution for site surveys.

The frequency spectra of these 2D site data are disappointingly low and the spectra narrow compared to that which might be expected from a dedicated site survey. For example, Sonnier & Gerlach (1999) suggest high-resolution site survey data can be obtained above 400 Hz. The low frequency content of these particular site survey data must be borne in mind when applying these results and observations to other site survey datasets which may contain higher frequencies.

## RESULTS AND IMPLEMENTATION

In the authors' view, work described above showed that the 3D data available within the deep-water WDDM area were of sufficient quality to replace existing quality 2D data. The loss of higher frequencies in the 3D data is more than outweighed by the benefits of denser spatial sampling, 3D migration, energy penetration, immediate availability and reduced cost. The spatial sampling of the 3D data in this area is particularly important given the high density of small gas accumulations.

Implementation of this recommendation involved presenting the technical results to the Operations and Drilling department within BG Group. Operations and Drilling buy-in was ensured by commissioning an independent contractor to audit both



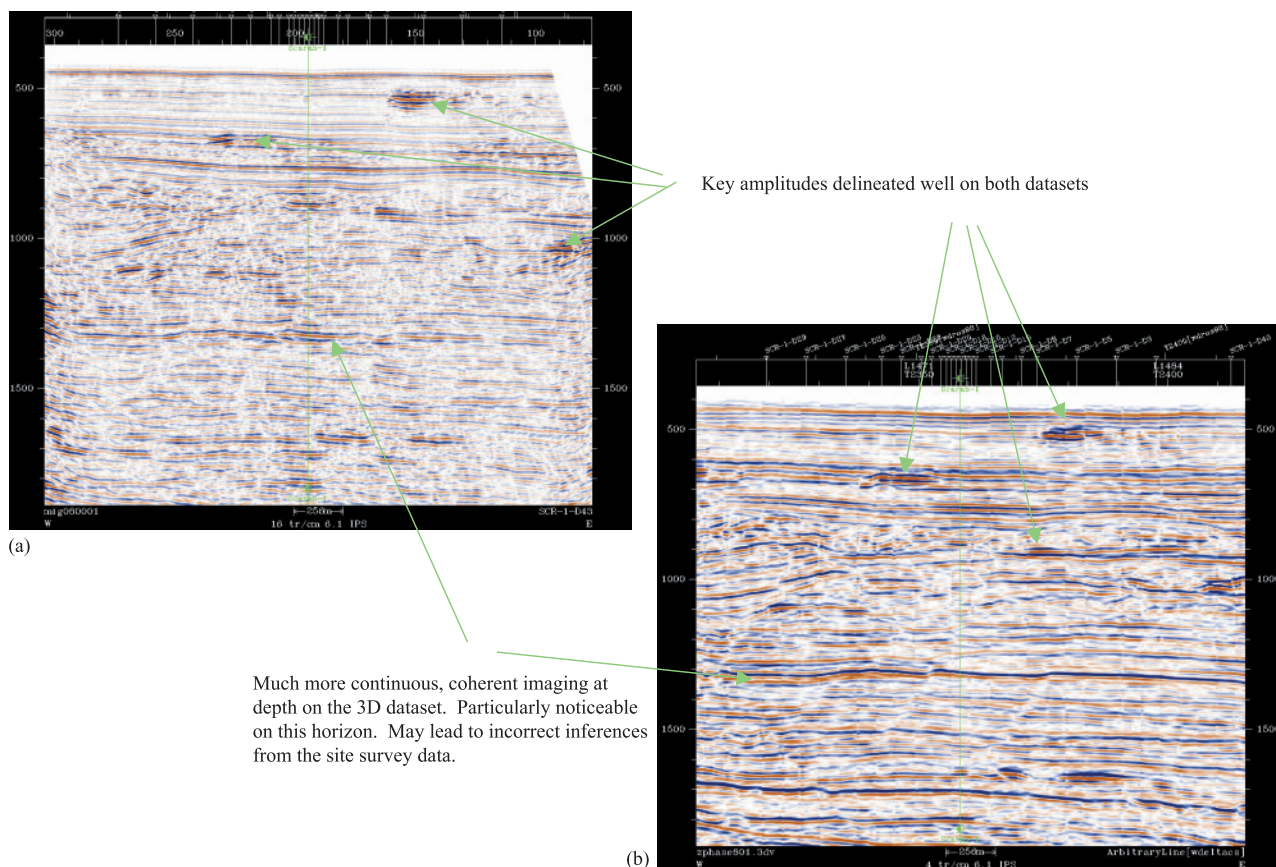


**Fig. 10.** (a) Scarab-1 2D data and (b) equivalent line from the 3D data volume. Areas of similarity and difference have been highlighted.

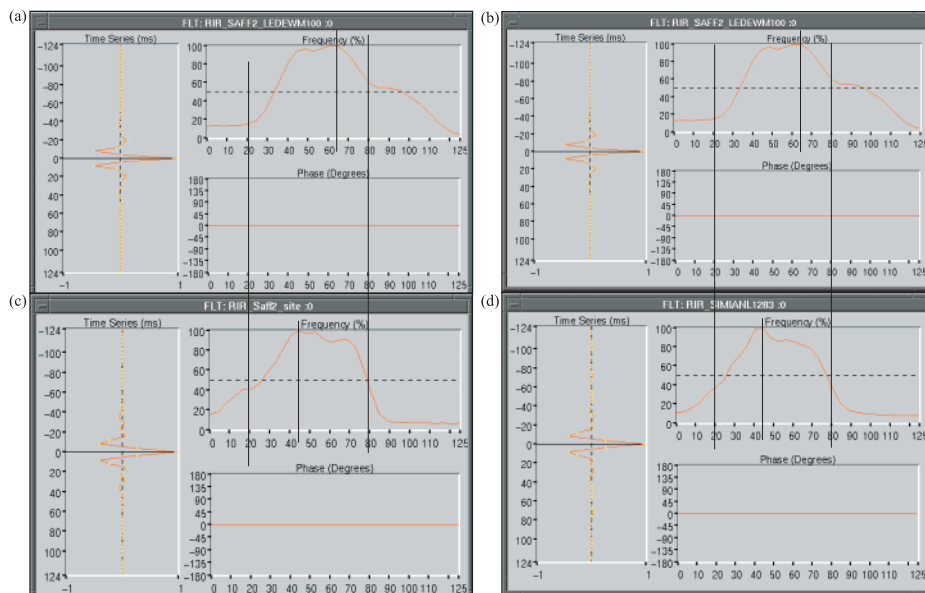


**Fig. 11.** Comparison of frequency spectra from (a, b) site survey data and (c) the 1996 3D site survey data, which includes the Scarab and Saffron wells. (d) The frequency spectra of the 1998 3D seismic data. The 1998 3D volume includes the Simian well and the future planned wells. Data extraction window 200–400 ms below mudline.

the workflow and conclusions reached. Following completion of this review, the independent auditors supported the conclusions and recommendations of this study. The insurers of the operating drilling rig were provided with summaries of the initial work and the independent audit. The recommendations of this study and the audit were accepted by the rig insurers and approval was given to go ahead with the 2000 drilling campaign using 3D data only, augmented by conventional analogue site survey data.

Following completion of the various steps outlined in the previous paragraph, the 2000 WDDM drilling campaign began without acquiring any digital site survey data and using only hazards mapped and prognosed from the 3D data. Five wells, Simian-2, -3, Sapphire-1, -2 and Sienna-1, were successfully drilled. All of these wells were drilled in a safe, efficient, effective fashion with no adverse operational impact from not acquiring any conventional 2D data. Using the exploration 3D data reduced environmental exposure because a shorter survey



time was required and also generated significant operational savings.

The authors would like to thank Rashid Petroleum Company, BG Group and Edison Gas for permission to publish this paper. This paper has been based on a significant amount of work that has been carried out on the West Delta Deep Marine Concession since it was awarded in 1995. In particular, contributions to this paper have been made by Magdi Abd El Hay, Sarah Brazier, Mark Cockram, Mohammed El Bedewi, Francesco Federici, Hossam Fathy, Kai Green, Mark Griffiths, Colin Harwood, Antony Lewis, Ramadan Ramadan and Howard Ryan. Thanks also go to Phil Wood and Rosie Kelly for reviewing and suggesting improvements in the preparation of this paper.

## REFERENCES

- Campbell, K.J. 1997. Fast-track development: The evolving role of 3D seismic data in deepwater hazards assessment and site investigation. Paper OTC 8306, presented at the Offshore Technology Conference, Houston, Texas, May 1997.
- Campbell, K.J. 1999. Deepwater geohazards: How significant are they? *The Leading Edge*, **18**, 514–519.
- Cowland, A.P. 1996. Drill site Geohazard Identification facilitated by rework of suitable existing 3D seismic data volumes. Paper OTC 7970, presented at the Offshore Technology Conference, Houston, Texas, May 1996.
- Haskell, N., Nissen, S. & Hughes, M. 1999. *et al.* Delineation of geologic drilling hazards using 3-D seismic attributes. *The Leading Edge*, **18**, 373–382.
- Hill, A.W. 1996. The Use of exploration 3D data in geohazard assessment: Where does the future lie? Paper OTC 7966, presented at the Offshore Technology Conference, Houston, Texas, May 1996.
- Long, D., Bulat, J. & Sankey, M. 1999. Regional images of the seabed derived from 3D exploration seismic data. *Proceedings of the AAPG International Conference and Exhibition*, Birmingham, UK, 323–327.
- Samuel, A., Kneller, B., Raslan, S., Sharp, A. & Parsons, C. 2003. Prolific Deep Marine Slope Channels of the Nile Delta, Egypt. *AAPG Bulletin*, **87**, 541–560.
- Sherriff, R.E. 1991. *Encyclopaedic Dictionary of Exploration Geophysics*. Society of Exploration Geophysicists, Tulsa, Oklahoma.
- Sonnier, C. & Gerlach, G. 1999. Deepwater hazard detection with high-resolution 3-D seismic. *Offshore*, Mardi issue, 54–55.
- UK Offshore Operators Association 2000. *Guidelines for the conduct of mobile drilling rig site investigations in deep water. Version 1.0*. UKOOA, London, UK.

Received 30 May 2003; revised typescript accepted 16 September 2003.